AD-A128 287 AN IMPROVED STRAIN HARDENING CHARACTERIZATION IN THE ADINA CODE USING THE..(U) ARMY ARMAMENT RESEARCH AND DEVELOPMENT COMMAND ABERDEEN PROVI.. A D GUPTA ET AL. 1/1

UNCLASSIFIED MAY 83 ARBRL-TR-02484 SBI-AD-F300 234 F/G 9/2 NL

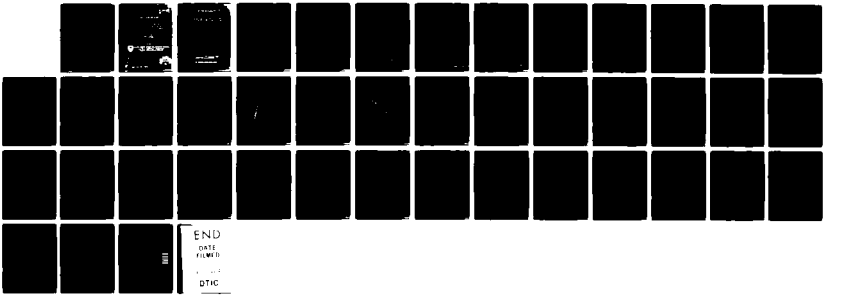

END
DATE FILMED
DTIC

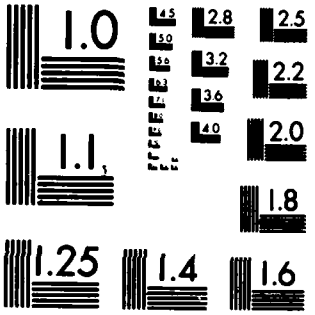

MICROCOPY RESOLUTION TEST CHART
NATIONAL BUREAU OF STANDARDS-1963-A

[redacted]

AN IMPROVED SINKIN MODELING CHARACTERIZATION IN THE ADINA CODE USING THE MECHANICAL SUBLAYER MODEL

Aaron D. Gupta
Joseph M. Santiago
Henry L. Wisniewski

May 1983

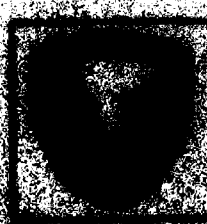

[redacted]

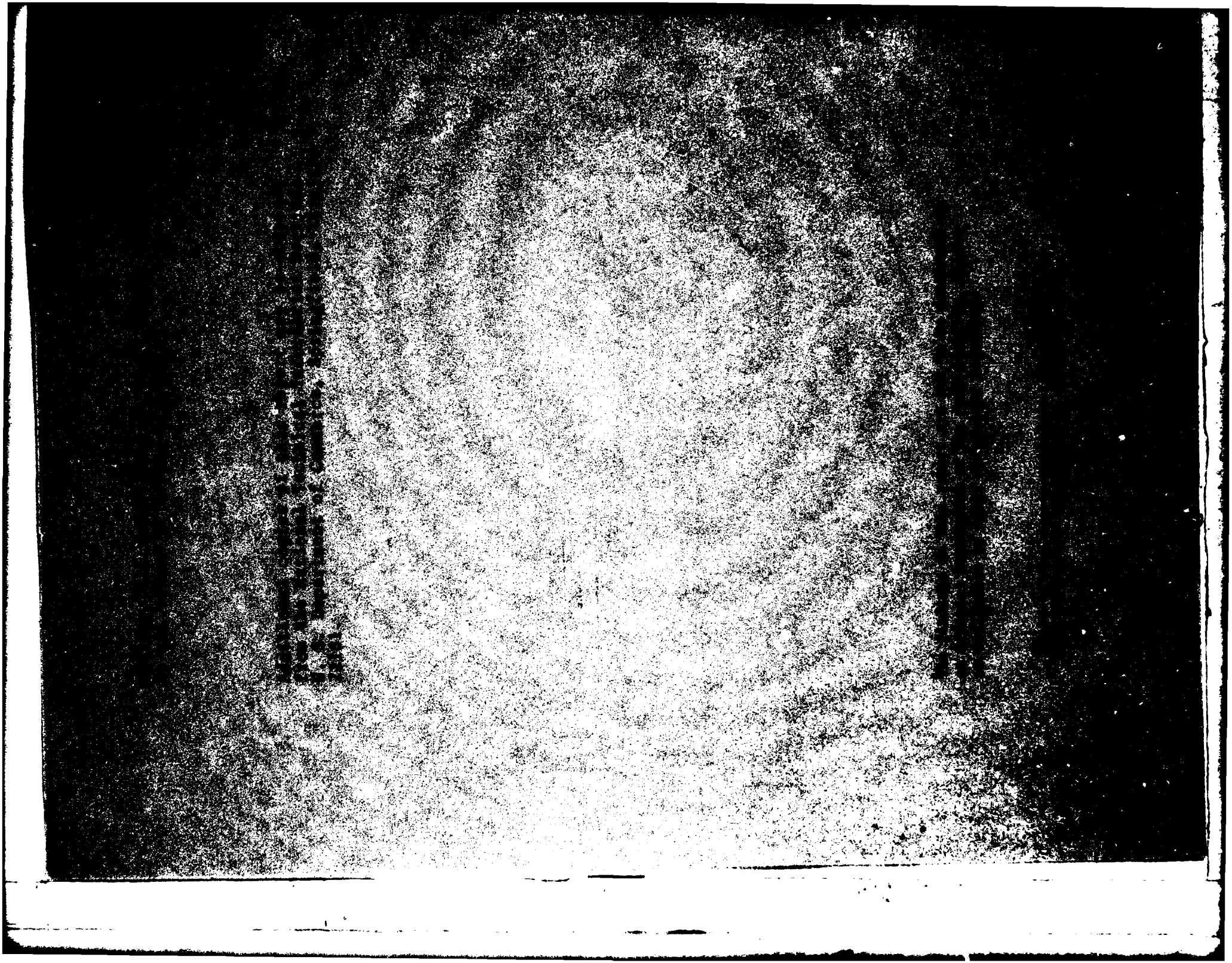

UNCLASSIFIED

SECURITY CLASSIFICATION OF THIS PAGE (When Data Entered)

REPORT DOCUMENTATION PAGE		READ INSTRUCTIONS BEFORE COMPLETING FORM
1. REPORT NUMBER TECHNICAL REPORT ARBRL-TR-02484	2. GOVT ACCESSION NO. AD-A128 287	3. RECIPIENT'S CATALOG NUMBER
4. TITLE (and Subtitle) AN IMPROVED STRAIN HARDENING CHARACTERIZATION IN THE ADINA CODE USING THE MECHANICAL SUBLAYER MODEL		5. TYPE OF REPORT & PERIOD COVERED Final 6. PERFORMING ORG. REPORT NUMBER
7. AUTHOR(s) Aaron D. Gupta Joseph M. Santiago Henry L. Wisniewski		8. CONTRACT OR GRANT NUMBER(s)
9. PERFORMING ORGANIZATION NAME AND ADDRESS US Army Ballistic Research Laboratory ATTN: DRDAR-BLT Aberdeen Proving Ground, MD 21005		10. PROGRAM ELEMENT, PROJECT, TASK AREA & WORK UNIT NUMBERS RDT&E 1L161102AH43
11. CONTROLLING OFFICE NAME AND ADDRESS USA Armament Research & Development Command US Army Ballistic Research Laboratory (DRDAR-BLA-S) Aberdeen Proving Ground, MD 21005		12. REPORT DATE May 1983 13. NUMBER OF PAGES 44
14. MONITORING AGENCY NAME & ADDRESS(if different from Controlling Office)		15. SECURITY CLASS. (of this report) UNCLASSIFIED 15a. DECLASSIFICATION/DOWNGRADING SCHEDULE

16. DISTRIBUTION STATEMENT (of this Report)

Approved for public release; distribution unlimited.

17. DISTRIBUTION STATEMENT (of the abstract entered in Block 20, if different from Report)

18. SUPPLEMENTARY NOTES

19. KEY WORDS (Continue on reverse side if necessary and identify by block number)

Finite Element Method
Structural Response Modeling
Nonlinear Strain Hardening
Prandtl-Reuss Plasticity Equations
Besseling-White Hardening Model
Mechanical Sublayer Model
Central Difference Time Integration

20. ABSTRACT (Continue on reverse side if necessary and identify by block number) jdk

The Besseling-White sublayer model for simulating the nonlinear strain hardening behavior of plastically deforming solids has been implemented in the ADINA finite element computer program as an additional material option. The Besseling-White model, also called the mechanical sublayer model, simulates strain hardening behavior by superposing the stresses from an array of elastic-perfectly plastic elements, called sublayers. Sublayer properties are determined from a polygonal fit to the stress-strain curve. This new material option

(Continued on reverse side)

DD FORM 1 JAN 73 1473 EDITION OF 1 NOV 65 IS OBSOLETE

Unclassified

SECURITY CLASSIFICATION OF THIS PAGE (When Data Entered)

Item 20. Continuation

has been validated by comparing predictions using this model and the two linear hardening models (kinematic and isotropic) presently in the standard version of ADINA. Comparison of predictions for the transverse deflection history of an impulsively loaded clamped-edge circular plate shows a close correlation between the sublayer model and the kinematic hardening model and a somewhat poorer, but still reasonable, correlation between the sublayer model and the isotropic hardening model.

TABLE OF CONTENTS

LIST OF ILLUSTRATIONS

I. INTRODUCTION

This investigation is part of an ongoing research program to improve the structural response modeling capabilities at the Terminal Ballistics Division of the Ballistic Research Laboratory. Among the computer programs used to model structural response at the BRL, the ADINA finite element code has been used intensively since its acquisition in 1978. It is a well documented[1,2,3] and widely used[4,5,6] general purpose program for calculating the static and dynamic responses of complex structures, with the capability of modeling both geometric and material nonlinearities. In particular, concerning the elastic-plastic behavior of materials, the code employs the Prandtl-Reuss theory of plastic flow[7] with either the von Mises yield condition or the Drucker-Prager yield condition. Using the von Mises condition, linear isotropic hardening or kinematic hardening can be modeled, while only elastic-perfectly plastic behavior can be modeled with the Drucker-Prager condition. Although linear hardening is adequate for situations where small amounts of plastic strain are involved, its use in predicting the large strain response of materials exhibiting nonlinear plastic behavior can result in considerable error. Hence, in order to improve the modeling of strain hardening in the ADINA code, the task of incorporating the Besseling-White sublayer model into the ADINA plasticity formulation was undertaken.

---

1. K.-J. Bathe, "ADINA - A Finite Element Program for Automatic Dynamic Incremental Nonlinear Analysis," Report 82448-1, Acoustic and Vibration Lab, MIT, Dept of Mechanical Engineering, Sep 75 (rev. Nov 79).

2. K.-J. Bathe, "Static and Dynamic Geometric and Material Nonlinear Analysis Using ADINA," Report 82448-2, Acoustic and Vibration Lab, MIT, Dept of Mechanical Engineering, May 76 (rev. May 77).

3. M.D. Snyder and K.-J. Bathe, "Formulation and Numerical Solution of Thermo-Elastic-Plastic and Creep Problems," Report 82448-3, Acoustic and Vibration Lab, MIT, Dept of Mechanical Engineering, Jun 77.

4. K.-J. Bathe (ed.), "Applications Using ADINA," Proceedings of the ADINA Conference August 1977, Report 82448-6, Acoustic and Vibration Lab, MIT, Dept of Mechanical Engineering, Aug 77.

5. K.-J. Bathe (ed.), "Nonlinear Finite Element Analysis and ADINA," Proceedings of the ADINA Conference August 1979, Report 82448-9, Acoustic and Vibration Lab, MIT, Dept of Mechanical Engineering, Aug 79.

6. K.-J. Bathe (ed.), "Nonlinear Finite Element Analysis and ADINA," Proceedings of the 3rd ADINA Conference, MIT, 10-12 Jun 81 or Computers & Structures, 13, No. 5-6, 1981.

7. R. Hill, The Mathematical Theory of Plasticity, Oxford University Press, London, 1950, pp. 38-45.

The Besseling-White model, also called the mechanical sublayer model, has been employed for some time in a number of structural response codes[8-11] and in particular in the PETROS series of shell response codes[12-15] developed for the BRL. This model simulates nonlinear strain hardening by summing the stresses from an array of elastic-perfectly plastic elements, called sublayers, for the material stress at a point. Nonlinear hardening is modeled in a piece-wise linear manner by each sublayer yielding at a different stress intensity, with the sublayer yield strength being determined by a polygonal fit to the uniaxial stress-strain curve.

---

8. H.A. Balmer and E.A. Witmer, "Theoretical-Experimental Correlation of Large Dynamic and Permanent Deformations of Impulsively-Loaded Simple Structures," Tech Docu Rpt No. FDL-TDR-64-108, Jul 64, Air Force Flight Dynamics Lab, Wright-Patterson AFB, Ohio.

9. J.M. Santiago, H.L. Wisniewski and N.J. Huffington, Jr., "A User's Manual for the REPSIL Code," BRL Rpt No. 1744, Oct 74, USA Ballistic Res Lab, APG, MD (AD A003176).

10. B. Hunsaker, Jr., D.K. Vaughn and J.A. Stricklin, "A Comparison of the Capability of Four Hardening Rules to Predict a Material's Plastic Behavior," Second National Congress on Pressure Vessels and Piping, ASME, San Francisco, CA, 23-27 Jun 75.

11. R.W.H. Wu and E.A. Witmer, "Analytical and Experimental Studies of Non-linear Transient Responses of Stiffened Cylindrical Panels," AIAA Journal, Vol. 13, No. 9, Sep 75, pp. 1171-1178.

12. L. Morino, J.W. Leech and E.A. Witmer, "PETROS 2: A Finite-Difference Method and Program for the Calculation of Large Elastic-Plastic Dynamically-Induced Deformation of Multilayer Variable-Thickness Shells" BRL Contract Rpt No.12, Dec 69, USA Ballistic Res Lab, APG, MD (AD 708774).

13. S. Atluri, E.A. Witmer, J.W. Leech and L. Morino, "PETROS 3: A Finite-Difference Method and Program for the Calculation of Large Elastic-Plastic Dynamically-Induced Deformations of Multilayer Variable-Thickness Shells," BRL Contract Rpt No. 60, Nov 71, USA Ballistic Res Lab, APG, MD (AD 890200L).

14. S.D. Pirotin, B.A. Berg and E.A. Witmer, "PETROS 3.5: New Developments and Program Manual for the Finite-Difference Calculation of Large Elastic-Plastic Transient Deformations of Multilayer Variable-Thickness Shells," BRL Contract Rpt No. 211, Feb 75, USA Ballistic Res Lab, APG, MD (AD A007215).

15. S.D. Pirotin, B.A. Berg and E.A. Witmer, "PETROS 4: New Developments and Program Manual for the Finite-Difference Calculation of Large Elastic-Plastic, and/or Viscoelastic Transient Deformations of Multilayer Variable-Thickness (1) Thin Hard-Bonded, (2) Moderately-Thick Hard-Bonded, or (3) Thin Soft-Bonded Shells," BRL Contract Rpt No. 316, Sep 76, USA Ballistic Res Lab, APG, MD (AD B014253L).

The sublayer model has been programmed in the ADINA code as an additional material option (model 12). Presently, it is available for use only with the explicit (central difference) time integration method. In order to insure that the sublayer model is correctly implemented in the code, parallel calculations have been performed using the sublayer model, the kinematic hardening model, and the isotropic hardening model to represent a linear strain hardening material. The correlation of deflections using the sublayer model and the kinematic hardening model is excellent. The correlation between the sublayer model and the isotropic hardening model although somewhat poor, as is to be expected, is still reasonable.

This report describes the formulation of the sublayer model and its implementation in the ADINA code. It also gives the results of the comparison between the sublayer model, the ADINA kinematic hardening model, and the ADINA isotropic hardening model. The material in this report has been published in preliminary form in the Proceedings of the First Chautauqua on Finite Element Modeling.[16]

II. FORMULATION OF THE MECHANICAL SUBLAYER MODEL

The Besseling-White or mechanical sublayer model originated with the concept by Duwez[17,18] of modeling nonlinear plastic hardening and unloading behavior by superposing the responses from a continuous aggregate of elastic-perfectly plastic elements. First, White[19] and then Besseling[20] in a more general setting extended Duwez's one-dimensional model to three dimensions and laid the basis for using the mechanical sublayer model as a computational procedure by proposing a discrete array of elements or sublayers. The computational use of the mechanical sublayer model was first carried out at MIT by Balmer and Witmer[8] in analyzing the response of structures using the finite difference method.

---

16. A.D. Gupta, J.M. Santiago and H.L. Wisniewski, "An Improved Strain Hardening Characterization in the ADINA Code Using the Mechanical Sublayer Concept," First Chautauqua on Finite Element Modeling, Harwichport, MA, 15-17 Sep 80, pp. 335-351.

17. P. Duwez, "On the Plasticity of Crystals," Physical Review, Vol. 47, 1935, pp. 494-501.

18. H.F. Bohnenblust and P. Duwez, "Some Properties of a Mechanical Model of Plasticity," J. Appl. Mech., Vol 15, 1948, pp. 222-225.

19. G.N. White, Jr., "Application of the Theory of Perfectly Plastic Solids to Stress Analysis of Strain Hardening Solids," Tech Report 51, Graduate Div of Applied Math., Brown University, Aug 50.

20. J.F. Besseling, "A Theory of Plastic Flow for Anisotropic Hardening in Plastic Deformation of an Initially Isotropic Material," Report S. 410, Nat. Aero. Rsch. Inst., Amsterdam (NLL), 1953.

The mechanical sublayer model assumes that the physical stress σ_{ij} at a point in the material can be decomposed into a weighted sum of N sublayer stresses σ^{α}_{ij} :

$$\sigma_{ij} = \sum_{\alpha=1}^{N} \omega^{\alpha} \sigma^{\alpha}_{ij} \qquad (1)$$

with ω^{α} the sublayer weighting factors. Sublayers are assumed to be elastic-perfectly plastic and to experience the same physical strain ε_{ij} . They share identical elastic constants, but have distinct values for their yield strengths. The values of sublayer yield strengths and weighting factors are determined from a polygonal fit to the uniaxial stress-strain curve (for example, see Figure 2), with the total number of sublayers N equal to the number of nonzero slope straight-line segments employed.

We can briefly describe how the sublayer model simulates nonlinear hardening by examining the case of uniaxial stress. Upon initial loading, all the sublayers respond elastically, but as loading proceeds sublayers will sequentially become plastic as they each reach their yield limit. Overall, this results in progressively diminishing values of the stress-strain modulus as the total stress increases, as illustrated in Figure 1. Upon unloading and reversal of loading, all the sublayers initially become elastic and remain elastic until the sublayer with the lowest yield stress again becomes plastic, whereupon the process repeats itself in the reverse direction, but with one significant difference: Straight-line segments are now twice the length of the corresponding segments on the initial loading curve due to each sublayer stress having to change from a given value of the yield stress to its negative value rather than from zero to the given value. Thus, the sublayer model exhibits a type of kinematic hardening behavior first proposed by Masing[21] that has subsequently achieved acceptance in modeling cyclic loading.[22,23]

---

21. G. Masing, "Eigenspannungen und Verfestigung beim Messing," Proceedings 2nd Intern. Congress for Appl. Mech., Zurich, Sep 1926.

22. Z. Mroz, "On the Description of Anisotropic Workhardening," J. Mech Phys Solids, Vol. 15, 1967, pp. 163-175.

23. Z. Mroz and N.C. Lind, "Simplified Theories of Cyclic Plasticity," Acta Mech., Vol. 22, 1975, pp. 131-152.

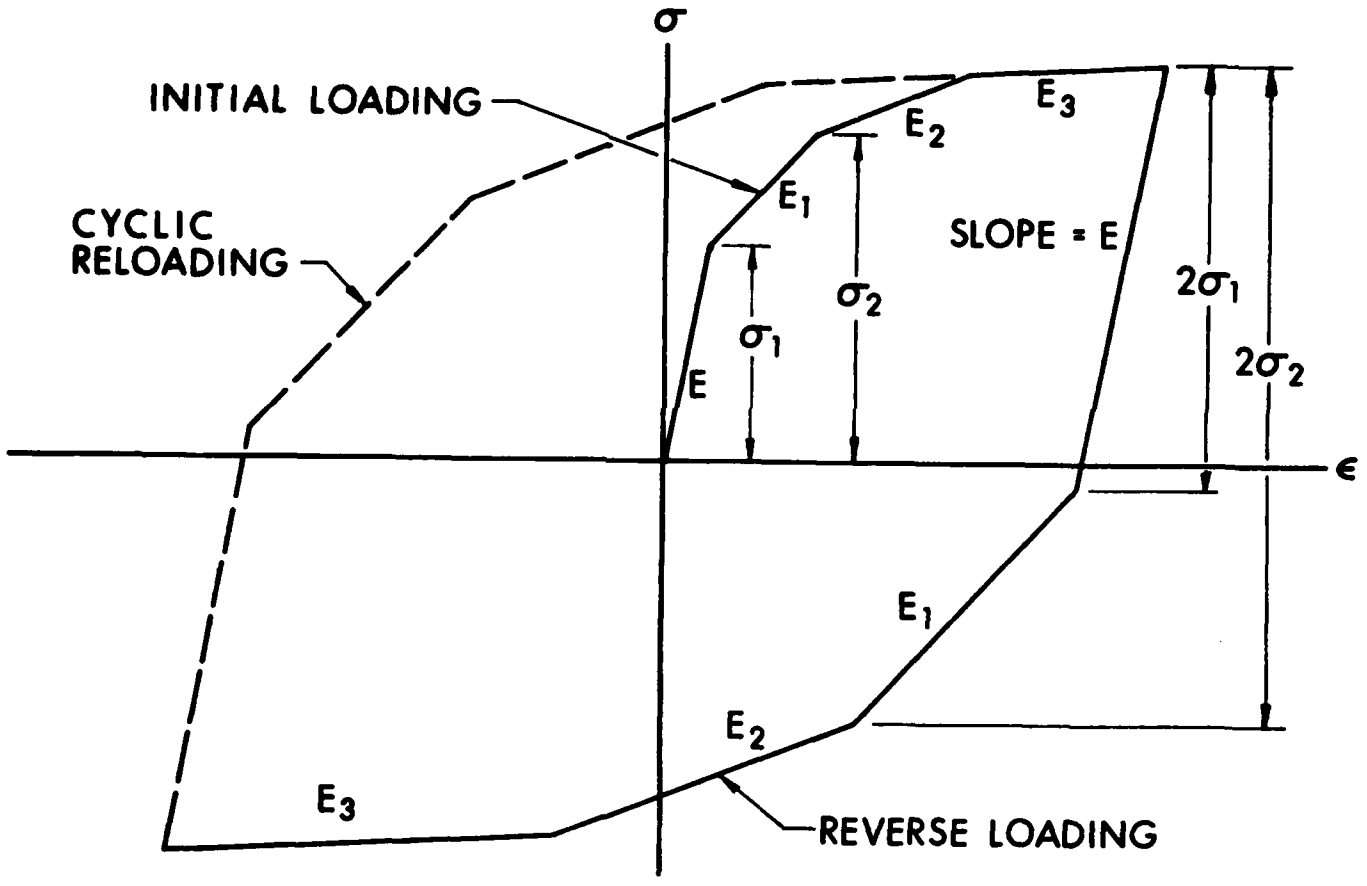

Figure 1. Mechanical sublayer modeling of the uniaxial s[illegible]urve upon initial loading and reversal of loadi[illegible].

A. Derivation of the Sublayer Equations

An incremental plasticity law is used to calculate the sublayer stresses. For a given sublayer α, the sublayer stress increment $\Delta\sigma_{ij}^{\alpha}$ is related to the elastic strain increment $\Delta\varepsilon_{ij}^{e\alpha}$ through the isotropic Hooke's law for the material,

$$\Delta\sigma_{ij}^{\alpha} = \frac{E}{1+\nu}\left[\Delta\varepsilon_{ij}^{e\alpha} + \frac{\nu}{1-2\nu}\,\Delta\varepsilon_{kk}^{e\alpha}\,\delta_{ij}\right] \tag{2}$$

where E is Young's modulus and ν is Poisson's ratio. The strain increment $\Delta\varepsilon_{ij}$ is the sum of the elastic sublayer strain increment $\Delta\varepsilon_{ij}^{e\alpha}$ and the plastic sublayer strain increment $\Delta\varepsilon_{ij}^{p\alpha}$,

$$\Delta\varepsilon_{ij} = \Delta\varepsilon_{ij}^{e\alpha} + \Delta\varepsilon_{ij}^{p\alpha} \tag{3}$$

where, as already mentioned, the total strain increment $\Delta\varepsilon_{ij}$ is the same for all sublayers at the point. Each sublayer is assumed to obey the von Mises yield condition:

$$S_{ij}^{\alpha}\,S_{ij}^{\alpha} = \frac{2}{3}\,(\sigma_{y}^{\alpha})^{2} \tag{4}$$

where σ_{y}^{α} is the sublayer yield stress and

$$S_{ij}^{\alpha} = \sigma_{ij}^{\alpha} - \frac{1}{3}\,\sigma_{kk}^{\alpha}\,\delta_{ij} \tag{5}$$

is the sublayer deviatoric stress. Should the material exhibit strain rate sensitivity, the yield stress for each sublayer can be made rate dependent through the relation

$$\sigma_{y}^{\alpha} = \sigma_{o}^{\alpha}\left[1 + (\dot{\epsilon}/D^{\alpha})^{1/N^{\alpha}}\right] \tag{6}$$

where σ_{o}^{α} is the static sublayer yield stress, $\dot{\epsilon}^{2}$ is the second invariant of the deviatoric strain rate tensor, and D^{α}, N^{α} are empirically determined constants[24] which generally are assumed to be identical for all sublayers. To complete the set of equations, the associative flow rule is appended in order to determine the plastic strain increment:

24. N. Perrone, "Response of Rate-Sensitive Frames to Impulsive Load," J. Engr. Mech. Div., ASCE Vol. 97, No. EM1, Proceedings Paper No. 7890, Feb 71.

$$\Delta\varepsilon_{ij}^{p\alpha} = \Delta\lambda^{\alpha} S_{ij}^{\alpha} \tag{7}$$

where $\Delta\lambda^{\alpha}$ is the usual plastic flow parameter that is adjusted to keep the stress state at the yield value. Combining equations (2), (3), and (6) we obtain the incremental equation used by the sublayer model to determine the sublayer stresses:

$$\Delta\sigma_{ij}^{\alpha} = \frac{E}{1+\nu}\left[\Delta\varepsilon_{ij} + \frac{\nu}{1-2\nu}\Delta\varepsilon_{kk}\,\delta_{ij}\right] - \Delta\tilde{\lambda}^{\alpha} S_{ij}^{\alpha} \tag{8}$$

where for convenience we replace $\Delta\lambda^{\alpha}$ by

$$\Delta\tilde{\lambda}^{\alpha} = \frac{E}{1+\nu}\Delta\lambda^{\alpha} \ . \tag{9}$$

Equations (1), (4), (5), (8), and, when treating a rate sensitive material, equation (6) are the basis for the mechanical sublayer plasticity calculation. When the sublayer stress rate lies inside the yield surface, as determined by (4), $\Delta\tilde{\lambda}^{\alpha}$ in (8) is set equal to zero; otherwise $\Delta\tilde{\lambda}^{\alpha}$ is determined by the requirement that the resulting stress state satisfy the yield condition. The details of determining the sublayer weighting factors ω^{α} and the static sublayer yield stresses σ_o^{α} from the polygonal fit to the uniaxial stress-strain curve are described in References 8 and 12.

B. Computational Procedure

The computational procedure assumes that at a given time step or cycle n in the code's computational algorithm the strain increments $\Delta\varepsilon_{ij}$ from the previous to the current cycle and the sublayer stresses $\sigma_{ij}^{\alpha}(n-1)$ at the previous cycle are known for all Gaussian integration points. Using this information the sublayer model computes first the current sublayer stresses $\sigma_{ij}^{\alpha}(n)$ and from these the current physical stresses $\sigma_{ij}(n)$ by means of the algorithm[25] which we now outline.

25. J.M. Santiago, "Formulation of the Large Deflection Shell Equations for Use in Finite-Difference Structural Response Codes," BRL Rpt No. 1571, Feb 72, USA Ballistic Res Lab, APG, MD (AD 740742).

Starting with the sublayer having the smallest value of the yield stress, a trial elastic stress increment $\Delta\sigma^{e}_{ij}$ is computed by assuming that no plastic flow occurs during the increment so that $\Delta\lambda^{\alpha} = 0$ and equation (8) becomes:

$$\Delta\sigma^{e}_{ij} = \frac{E}{1+\nu} \left[\Delta\varepsilon_{ij} + \frac{\nu}{1-2\nu} \Delta\varepsilon_{kk} \delta_{ij} \right] . \qquad (10)$$

Adding the elastic stress increment to the previous sublayer stress, a trial sublayer stress for the current cycle is obtained

$$\sigma^{T\alpha}_{ij} = \sigma^{\alpha}_{ij}(n-1) + \Delta\sigma^{e}_{ij} . \qquad (11)$$

Writing the von Mises yield function for the sublayer as

$$\phi^{\alpha}(\sigma^{\alpha}_{ij}) = \sigma^{\alpha}_{ij}\,\sigma^{\alpha}_{ij} - \frac{1}{3}\,(\sigma^{\alpha}_{kk})^{2} - \frac{2}{3}\,(\sigma^{\alpha}_{y})^{2} \qquad (12)$$

the trial sublayer stress is checked by substitution in the von Mises yield. If $\phi^{\alpha}(\sigma^{T\alpha}_{ij}) \leq 0$, then the addition of the elastic stress increment $\Delta\sigma^{e}_{ij}$ results in a stress state inside or on the yield surface, and hence the trial sublayer stress has given the correct sublayer stress for the current cycle:

$$\sigma^{\alpha}_{ij}(n) = \sigma^{T\alpha}_{ij} . \qquad (13)$$

If, however, $\phi^{\alpha}(\sigma^{T\alpha}_{ij}) > 0$, then yielding occurs, and according to (8) the trial sublayer stress needs to be corrected to obtain the current sublayer stress:

$$\sigma^{\alpha}_{ij}(n) = \sigma^{T\alpha}_{ij} - \Delta\tilde{\lambda}^{\alpha}\, S^{\alpha}_{ij}(n-1) . \qquad (14)$$

To determine the flow parameter $\Delta\tilde{\lambda}^{\alpha}$, equation (14) is inserted in the von Mises yield function (12) and, in order to insure that the resulting sublayer stress state is on the yield surface, the function is set equal to zero; i.e., $\phi^{\alpha}(\sigma^{\alpha}_{ij}(n)) = 0$. This determines a quadratic equation in $\Delta\tilde{\lambda}^{\alpha}$ (Reference 25), which is solved for the smallest positive root:

$$\Delta\tilde{\lambda}^{\alpha} = \frac{B}{A} - \left[\left(\frac{B}{A}\right)^2 - \frac{C}{A}\right]^{\frac{1}{2}} \qquad (15)$$

where

$$A = S^{\alpha}_{ij}(n\text{-}1)\ S^{\alpha}_{ij}(n\text{-}1)$$

$$B = \overset{T\alpha}{\sigma}_{ij}\ S^{\alpha}_{ij}(n\text{-}1)$$

$$C = \phi^{\alpha}(\overset{T\alpha}{\sigma}_{ij}) \ .$$

In some instances when the strain increment is too large, the discriminant under the radical in equation (15) can become negative due to the trial sublayer stress causing a state too far outside the yield surface. In such instances a subincremental iterative procedure described in Reference 9 is employed to reduce the strain increment to a number of subincrements in order to obtain a real solution for $\Delta\tilde{\lambda}^{\alpha}$.

Once the plastic flow parameter $\Delta\tilde{\lambda}^{\alpha}$ is determined, the sublayer stress $\sigma^{\alpha}_{ij}(n)$ is computed from (14) and is stored for the next computational cycle. This procedure is repeated until all the current sublayer stresses at the given integration point are found, and then these are summed with the appropriate weighting factors to determine the physical stress at that point for the current cycle

$$\sigma_{ij}(n) = \sum_{\alpha=1}^{N} \omega^{\alpha}\ \sigma^{\alpha}_{ij}(n) \ . \qquad (16)$$

C. Program Implementation

The ADINA code is structured to accept nonlinear material models not currently included in the material library. No changes to the program are necessary except for inserting the user supplied material model subroutine in terms of the appropriate source program call variables described in Reference 1.

The sublayer model has been inserted as material model 12 (subroutine EL3D12), which is intended for triaxial states of stress. As presently programmed the sublayer model can only be used for explicit time integration. The subroutine calculates the current stresses from the strain increments and the previous stresses as explained earlier, but has not as yet been programmed to calculate the stress-strain matrix (subroutine MIDEP3) needed to determine the stiffness matrix required for implicit time integration. Because the sublayer stresses at each cycle must be stored in order to perform the stress calculation for the subsequent cycle, provision for storage must be made in accordance with the number of sublayers used. This means that when more than one sublayer is employed the sublayer model will require more storage than the ADINA kinematic hardening model.

III. DYNAMIC RESPONSE ANALYSIS OF PLATE

In order to evaluate the ability of the mechanical sublayer model as implemented in the ADINA code to reproduce the dynamic response of structures with nonlinear material characteristics, calculations have been undertaken to compare code predictions with known experimental results. Some preliminary results from this investigation are now available concerning a comparison between the sublayer model and the existing ADINA hardening models. Employing each plasticity model, the code was used to solve a problem involving the large transient deflection of an impulsively loaded, clamped-edge, circular flat plate.

The problem is taken from an experimental report[26] and concerns a plate 6.35mm thick with a radius of 63.5mm, made of 2024-0 aluminum. This material exhibits a considerable degree of nonlinear hardening which can be closely approximated by the sublayer model as illustrated in Figure 2.

However, for purposes of comparing the sublayer model (model 12) to the isotropic hardening model (model 8) and the kinematic hardening model (model 9), we need only consider the following material responses: purely elastic, elastic-perfectly plastic, and elastic-linear strain hardening. Hence, for this purpose the following values of the material properties were used:

σ_y	(yield stress	= 85.5 MPa
E	(Young's modulus)	= 73.7 GPa
E_T	(strain hardening modulus)	= 6.85 GPa
ν	(Poisson's ratio)	= 1/3
ρ	(mass density)	= 2775 Kg/m^3

The deformation was initiated by subjecting the plate to a uniform impulse velocity of 53.09 m/s.

26. E.A. Witmer, F. Merlis and S.D. Pirotin, "Experimental Studies of Explosively-Induced Large Deformations of Flat Circular 2024-0 Aluminum Plates with Clamped Edges and of Free Thin Cylindrical 6061-T6 Shells," BRL Contract Rpt No. 134, Jan 74, USA Ballistic Res Lab, APG, MD (AD 917518L).

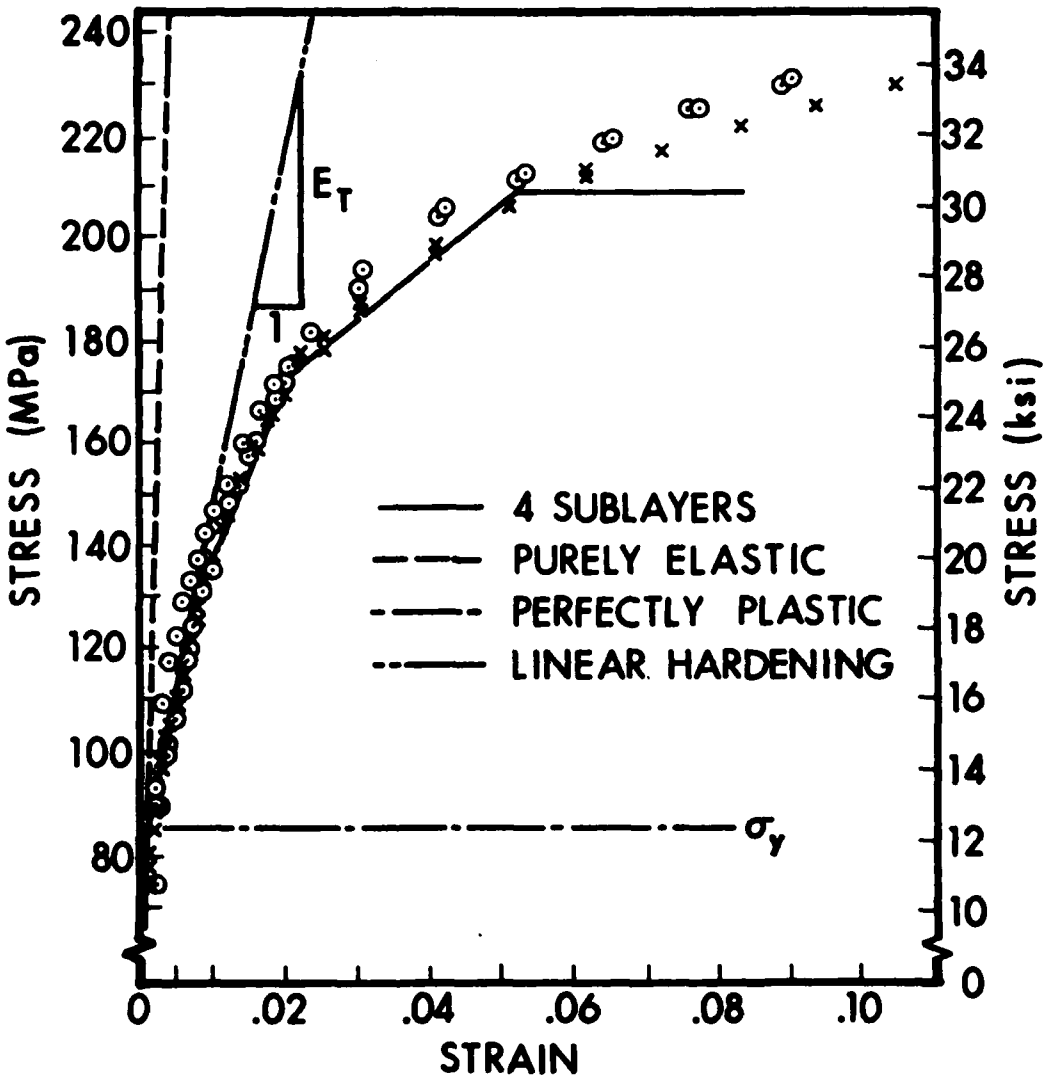

Figure 2. Tensile uniaxial stress-strain data for 2024-0 aluminum taken from Reference 26 approximated by a number of material response representations.

By passing a symmetry plane through a diameter, only half the plate had to be treated. Twenty 3-dimensional brick elements were used to model half the plate, as illustrated in Figure 3. Each element used 16 nodes except for those bounding the pole which used only 12 nodes, giving a total of 142 nodes for the problem. Two Gaussian integration points were employed along each coordinate direction, making a total of eight points per element. All nodes along the circular boundary were assumed to be fixed. Explicit time integration was used for all calculations and the total Lagrangian formulation was used for the nonlinear geometric analysis.

A. Elastic Comparison

The purely elastic response was modeled by increasing the value of the yield stress σ_y to a level insuring elastic behavior only. (See Figure 2.) The elastic calculations were performed using first a linear and then a nonlinear geometric analysis.

For the linear analysis, the elastic response of the sublayer model (model 12) was compared with the response of the ADINA linear analysis model (model 1) and the elastic response of the ADINA strain hardening model (either model 8 or 9, since the isotropic and kinematic models coincide for elastic response). The numerical results from the three models were found to coincide exactly. This is illustrated in Figure 4 for the history of the deflection at the pole.

For the geometric nonlinear analysis the elastic responses of the sublayer model and the strain hardening model were compared. Again, it was found that the models gave coincident numerical results, as shown in Figure 4.

Hence for both linear and nonlinear geometric analyses, the sublayer model and the ADINA models are elastically consistent. Moreover, it is observed that for the given problem, nonlinear geometric effects are already substantial at levels of maximum deflection in the order of 60% of the plate thickness.

B. Elastic-Perfectly Plastic Comparison

For the elastic-perfectly plastic comparison, the yield stress was returned to the value of $\sigma_y = 85.5$ MPa and the strain hardening modulus E_T was set equal to zero, as shown in Figure 2. The sublayer model (with only one sublayer), the isotropic hardening model, and the kinematic hardening model were compared using the nonlinear geometric analysis.

Excellent correlation between the results of the three models was found although they no longer coincided numerically. As portrayed in Figure 4, the deflection history curves for the models overlap. Hence, for elastic-perfectly plastic behavior, the sublayer model and the ADINA plasticity models give the same results physically. Also, comparing the elastic-perfectly plastic response with the purely elastic response, we see the dissipative effects of plastic flow in the reduced and smoothed deflection peaks at late times.

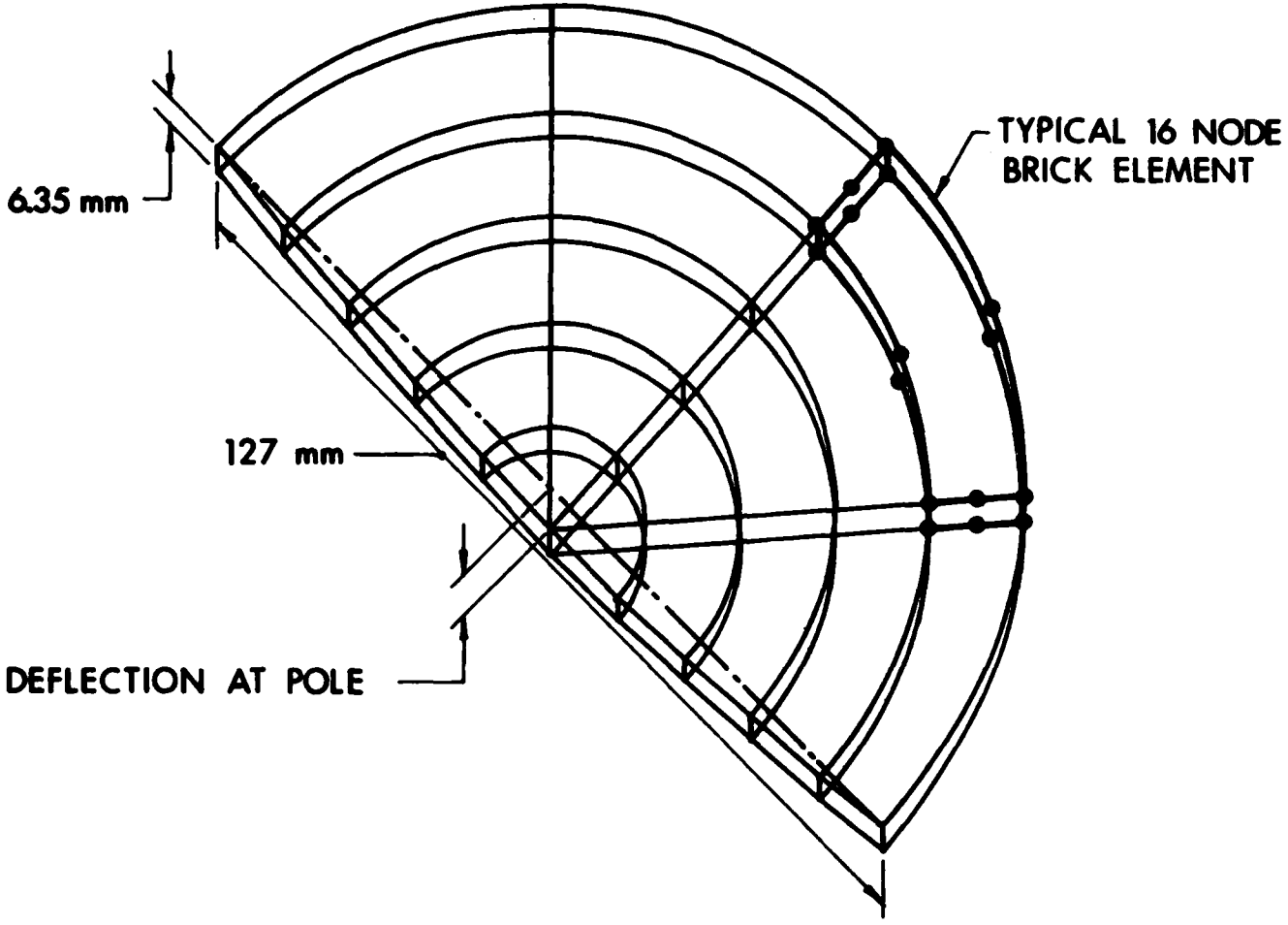

Figure 3. Finite element modeling of half the plate showing a typical element and the direction of polar deflection.

C. Elastic-Linear Strain Hardening Comparison

To model strain hardening behavior, the strain hardening modulus was reset at the value of E_T = 6.85 GPa. Two sublayers were used with the yield stress of the second sublayer raised to a value high enough to insure its elastic behavior, so that only the first sublayer could become plastic. This insured that the sublayer model would exhibit linear hardening behavior, so that a meaningful comparison could be made with the standard ADINA models. The nonlinear geometric analysis option was used for the comparison.

The correlation between deflections from the sublayer model and the kinematic hardening model is still very good, as illustrated in Figure 5, but the curves no longer overlap as they did for the perfectly plastic case. The agreement between the values of the stress components at Gaussian integration points ranged in the order of one to three significant figures.

On the other hand, the deflection using the isotropic hardening model was only in fair agreement with the deflections from the other two models, although still physically acceptable. However, this is hardly surprising since the isotropic model bases its plasticity calculation on the concept of an expanding yield surface rather than a shifting yield surface as do the other models. Hence, whenever a significant amount of plastic flow reversal occurs, the models can be expected to predict different responses.

Calculations were also performed using four sublayers to model the stress-strain curve as shown in Figure 2. However, for the level of loading imposed on the plate, most of the plastic flow was experienced by the first sublayer, so that the results were graphically indistinguishable from those of the two-sublayer model.

IV. CONCLUSIONS

The mechanical sublayer model has been implemented in the ADINA finite element structural response code, extending its capability to model elastoplastic constitutive behavior to nonlinear kinematically hardening materials. The model is formulated to treat triaxial states of stress. It is currently programmed for use in both the linear and nonlinear geometric analyses of transient response employing explicit time integration. The sublayer model subroutine has been exercised, and calculations using the sublayer model and the standard ADINA hardening models show that results are in close agreement and appear physically reasonable.

A sublayer model for biaxial states of stress is currently being devised to treat plane stress problems. When ready, this model will also be implemented in the code. It now appears that the sublayer model can be easily reformulated to permit implicit time integration. Further effort is underway to validate the model with available experimental results and with predictions from reliable finite difference response codes, such as REPSIL[9] and PETROS[14,15] Eventually, the sublayer model can be expected to replace the existing kinematic hardening model, thereby considerably extending the material modeling capabilities of the ADINA code.

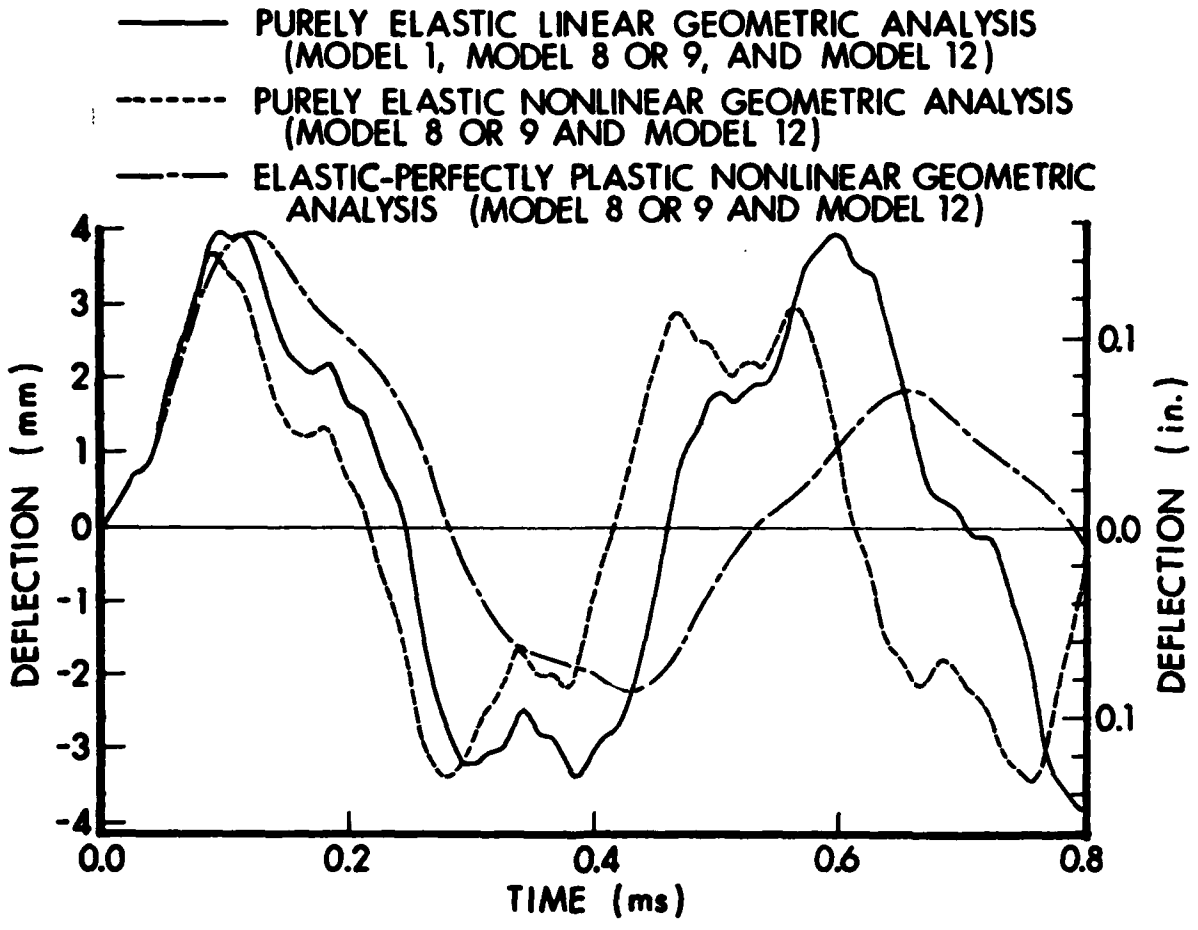

Figure 4. Comparison of the deflection histories at the pole for purely elastic responses and an elastic-perfectly plastic response.

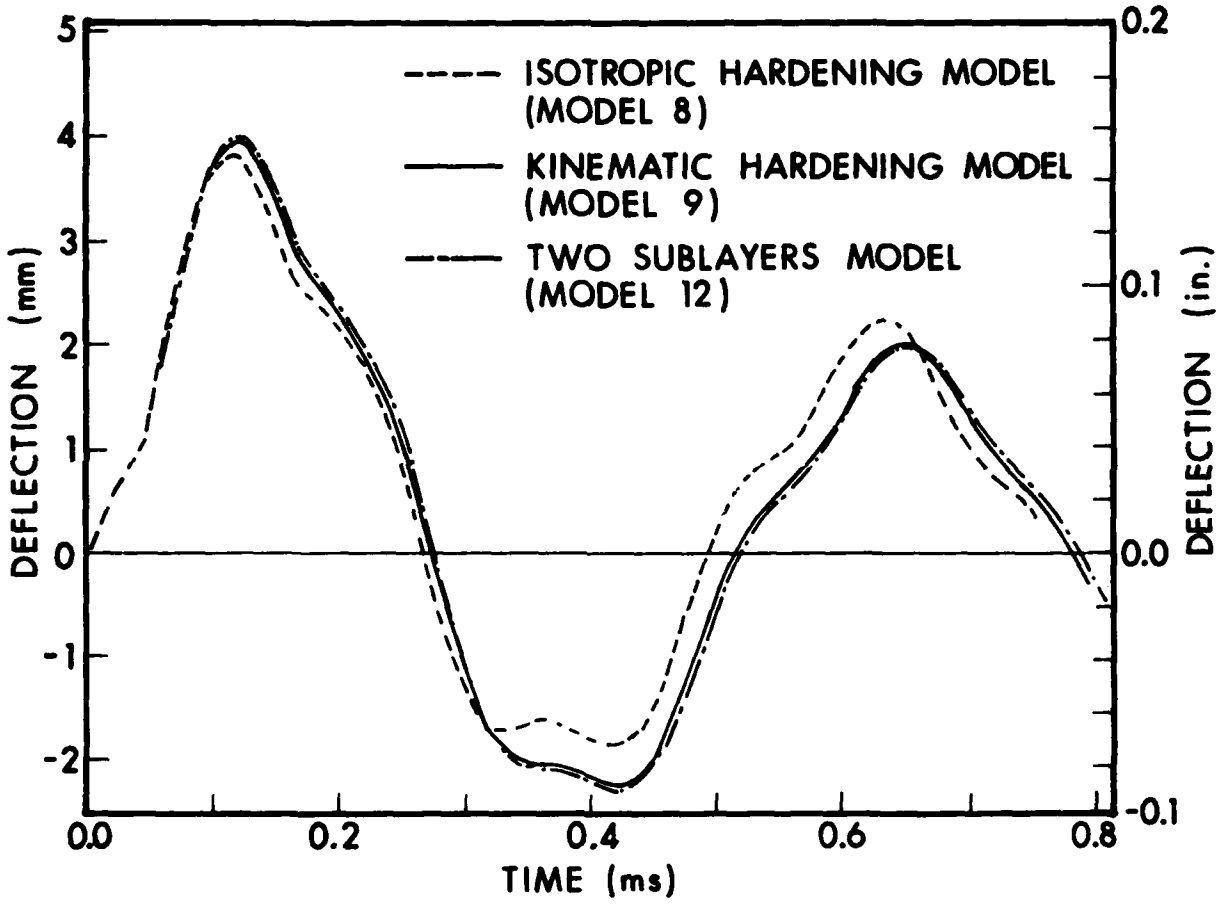

Figure 5. Comparison of the deflection histories at the pole for an elastic-linear hardening response using the isotropic hardening, kinematic hardening, and sublayer models.

REFERENCES

1. K.-J. Bathe, "ADINA - A Finite Element Program for Automatic Dynamic Incremental Nonlinear Analysis," Report 82448-1, Acoustic and Vibration Lab, MIT, Dept of Mechanical Engineering, Sep 75 (rev. Nov 79).

2. K.-J. Bathe, "Static and Dynamic Geometric and Material Nonlinear Analysis Using ADINA," Report 82448-2, Acoustic and Vibration Lab, MIT, Dept of Mechanical Engineering, May 76 (rev. May 77).

3. M.D. Snyder and K.-J. Bathe, "Formulation and Numerical Solution of Thermo-Elastic-Plastic and Creep Problems," Report 82448-3, Acoustic and Vibration Lab, MIT, Dept of Mechanical Engineering, Jun 77.

4. K.-J. Bathe (ed.), "Applications Using ADINA," Proceedings of the ADINA Conference August 1977, Report 82448-6, Acoustic and Vibration Lab, MIT, Dept of Mechanical Engineering, Aug 77.

5. K.-J. Bathe (ed.), "Nonlinear Finite Element Analysis and ADINA," Proceedings of the ADINA Conference August 1979, Report 82448-9, Acoustic and Vibration Lab, MIT, Dept of Mechanical Engineering, Aug 79.

6. K.-J. Bathe (ed.), "Nonlinear Finite Element Analysis and ADINA," Proceedings of the 3rd ADINA Conference, MIT, 10-12 Jun 81 or Computers & Structures, 13, No. 5-6, 1981.

7. R. Hill, The Mathematical Theory of Plasticity, Oxford University Press, London, 1950, pp. 38-45.

8. H.A. Balmer and E.A. Witmer, "Theoretical-Experimental Correlation of Large Dynamic and Permanent Deformations of Impulsively-Loaded Simple Structures," Tech Docu Rpt No. FDL-TDR-64-108, Jul 64, Air Force Flight Dynamics Lab, Wright-Patterson AFB, Ohio.

9. J.M. Santiago, H.L. Wisniewski and N.J. Huffington, Jr., "A User's Manual for the REPSIL Code," BRL Rpt No. 1744, Oct 74, USA Ballistic Research Lab, APG, MD (AD A003176).

10. B. Hunsaker, Jr., D.K. Vaughn and J.A. Stricklin, "A Comparison of the Capability of Four Hardening Rules to Predict a Material's Plastic Behavior," Second National Congress on Pressure Vessels and Piping, ASME, San Francisco, CA, 23-27 Jun 75.

11. R.W.H. Wu and E.A. Witmer, "Analytical and Experimental Studies of Nonlinear Transient Responses of Stiffened Cylindrical Panels," AIAA Journal, Vol. 13, No. 9, Sep 75, pp. 1171-1178.

12. L. Morino, J.W. Leech and E.A. Witmer, "PETROS 2: A Finite-Difference Method and Program for the Calculation of Large Elastic-Plastic Dynamically-Induced Deformation of Multilayer Variable-Thickness Shells," BRL Contract Rpt No.12, Dec 69, USA Ballistic Res Lab, APG, MD (AD 708774).

13. S. Atluri, E.A. Witmer, J.W. Leech and L. Morino, "PETROS 3: A Finite-Difference Method and Program for the Calculation of Large Elastic-Plastic Dynamically-Induced Deformations of Multilayer Variable-Thickness Shells," BRL Contract Rpt No. 60, Nov 71, USA Ballistic Res Lab, APG, MD (AD 890200L).

14. S.D. Pirotin, B.A. Berg and E.A. Witmer, "PETROS 3.5: New Developments and Program Manual for the Finite-Difference Calculation of Large Elastic-Plastic Transient Deformations of Multilayer Variable-Thickness Shells," BRL Contract Rpt No. 211, Feb 75, USA Ballistic Res Lab, APG, MD (AD A007215).

15. S.D. Pirotin, B.A. Berg and E.A. Witmer, "PETROS 4: New Developments and Program Manual for the Finite-Difference Calculation of Large Elastic-Plastic, and/or Viscoelastic Transient Deformations of Multilayer Variable-Thickness (1) Thin Hard-Bonded, (2) Moderately-Thick Hard-Bonded, or (3) Thin Soft-Bonded Shells," BRL Contract Rpt No. 316, Sep 76, USA Ballistic Res Lab, APG, MD (AD B014253L).

16. A.D. Gupta, J.M. Santiago and H.L. Wisniewski, "An Improved Strain Hardening Characterization in the ADINA Code Using the Mechanical Sub-layer Concept," First Chautauqua on Finite Element Modeling, Harwichport MA, 15-17 Sep 80, pp. 335-351.

17. P. Duwez, "On the Plasticity of Crystals," Physical Review, Vol. 47, 1935, pp. 494-501.

18. H.F. Bohnenblust and P. Duwez, "Some Properties of a Mechanical Model of Plasticity," J. Appl. Mech., Vol 15, 1948, pp. 222-225.

19. G.N. White, Jr., "Application of the Theory of Perfectly Plastic Solids to Stress Analysis of Strain Hardening Solids," Tech Report 51, Graduate Div of Applied Math., Brown University, Aug 50.

20. J.F. Besseling, "A Theory of Plastic Flow for Anisotropic Hardening in Plastic Deformation of an Initially Isotropic Material," Report S. 410, Nat. Aero. Rsch. Inst., Amsterdam (NLL), 1953.

21. G. Masing, "Eigenspannungen und Verfestigung beim Messing," Proceedings 2nd Intern. Congress for Appl. Mech., Zurich, Sep 1926.

22. Z. Mroz, "On the Description of Anisotropic Workhardening," J. Mech Phys Solids, Vol. 15, 1967, pp. 163-175.

23. Z. Mroz and N.C. Lind, "Simplified Theories of Cyclic Plasticity," Acta Mech., Vol. 22, 1975, pp. 131-152.

24. N. Perrone, "Response of Rate-Sensitive Frames to Impulsive Load," J. Engr. Mech. Div., ASCE Vol. 97, No. EM1, Proceedings Paper No. 7890, Feb 71.

25. J.M. Santiago, "Formulation of the Large Deflection Shell Equations for Use in Finite-Difference Structural Response Codes," BRL Rpt No. 1571, Feb 72, USA Ballistic Res Lab, APG, MD (AD 740742).

26. E.A. Witmer, F. Merlis and S.D. Pirotin, "Experimental Studies of Explosively-Induced Large Deformations of Flat Circular 2024-0 Aluminum Plates with Clamped Edges and of Free Thin Cylindrical 6061-T6 Shells," BRL Contract Rpt No. 134, Jan 74, USA Ballistic Res Lab, APG, MD (AD 917518L).

APPENDIX A

PROGRAM LISTING OF SUBLAYER MODEL SUBROUTINE

1. Element Group Control Card (20I4) Page X.5 (Ref. 1)

	Columns	Variable	
Model	57-60	NPAR(15)	12, for sublayer model
NCON	65-68	NPAR(17)	2, for sublayer model
IDW	77-80	NPAR(20)	(Number of sublayers x 6) + 7

2. Material Property Data Cards Page X.11 (Ref. 1)

   a. Material number card

      No change

   b. Material Property Card Page X.11 (Ref. 1)

Columns	Variable	
1-10	PROP(1,N)	Young's modulus, E
11-20	PROP(2,N)	Poisson's ratio, ν

3. Sublayer Data

   a. (NSUBL(ILAY), ILAY = 1,NUMMAT) (16I5)

      where

      NSUBL(ILAY) = the number of sublayers in layer ILAY.

      NUMMAT = NPAR(16) Number of different sets of material properties.

   b. (SIG,DZ(ILAY,ISB), ISD = 1,NSBL) (5E15.6)

      ISG,DZ = the magnitude of the ordinate of the 1-dimensional stress-strain curve.

      NSBL = Number of sublayers in the layer (material) in question.

      ILAY = Material in question.

   c. (EPS,DZ(ILAY,ISB), ISB=1, NSBL) (5E15.6)

      EPS,DZ = the magnitude of the abscissa of the 1-dimensional stress-strain curve.

      NSBL = Number of sublayers in the layer (material) in question.

```
C          EVALUATE STRESS INCREMENTS AND STRESSES
C                          MODEL=12
C     THE FOLLOWING VARIABLES ARE USED IN THIS SUBROUTINE
C
C        SIG      PREVIOUS STRESSES
C        EPS      PREVIOUS STRAINS
C
C        STRESS   CURRENT STRESSES (TO BE CALCULATED)
C        STRAIN   CURRENT STRAINS  (G I V E N)
C        IPEL     = 1, MATERIAL ELASTIC (INITIAL VALUE)
C                 = 2, MATERIAL PLASTIC
C        DELEPS   INCREMENTAL STRAINS
C        DELSIG   INCREMENTAL STRESSES, CALCULATED ON THE ASSUMPTION
C                 OF ELASTIC BEHAVIOR DURING STRAIN INCREMENT (DELEPS)
C          L      NO. OF SUB-INCREMENTS
C          LC     CHECK ON SUB-INCREMENTS
C        PROP(1)  YOUNGS MODULUS
C        PROP(2)  POISSONS RATIO
C        TR       TRIAL STRESSES
C        TC       CORRECTOR STRESSES
C        TM       STRESS PER/SUBLAYER
      DIMENSION PROP(1),EPS(1),SIG(NSBL,6)
      COMMON /EL/ IND,ICOUNT,NPAR(20),NUMEG,NEGL,NEGNL,IMASS,IDAMP,
     1            ISTAT,NDOF,KLIN,IEIG,IMASSN,IDAMPN
      COMMON /VAR/ NG,MODEX,IUPDT,KSTEP,ITEMAX,IEQREF,ITE,KPRI,
     1             IREF,IEQUIT,IPRI,KPLOTN,KPLOTE
      COMMON /MTMD3D/ D(36),STRESS(6),STRAIN(6),IPT,NEL,IPS
      COMMON /MATER/ COEFF(6),SIGMA(6),EEET(6)
      COMMON /MATEPI/ NSUBL(4),SIG1DZ(4,5),EPS1DZ(4,5)
      COMMON /DISDR/ DISD(9)
      COMMON /ELSTP/ TIME,IDTHF
      DIMENSION DELSIG(6),DELEPS(6),TR(6),TC(6),TM(6),STATE(2)
      EQUIVALENCE (NPAR(3),INDNL)
      DATA STATE /2H E,2H*P/
C
      IPELD=IPEL
      IF(IPT .NE. 1)GOTO 30
C     .....  CALCULATION OF MATERIAL CONSTANTS   ..................
      YM=PROP(1)
      PV=PROP(2)
      CALL MATPRO (MATP,PROP)
      SIGM=SIGMA(1)
C
      FACTOR=1.
      A1=YM/(1.+PV)
      C1=A1/2.
      A1=A1/(1.-2.*PV)
      B1=A1*PV
      A1=A1-B1
C        1. CALCULATE INCREMENTAL STRAINS
C
   30 DO 32 I=1,6
      STRESS(I)=0.0
   32 CONTINUE
```

```
      IF(INDNL .EQ. 3)GOTO 36
C                    TOTAL LAGRANGIAN
      DO 34 I=1,6
   34 DELEPS(I)=STRAIN(I)-EPS(I)
      GOTO 40
C                    UPDATED LAGRANGIAN
   36 DO 38 I=1,6
   38 DELEPS(I)=STRAIN(I)
C
   40 IPLAST=0
      DO 250 ISB=1,NSBL
C        STRESS PER SUBLAYER SIG(ISB,I)
      DO 43 I=1,6
      TM(I)=SIG(ISB,I)
   43 CONTINUE
C        KPRI=0 SKIP CALCULATION JUST PRINT STRESS
      IF(KPRI .EQ. 0)GOTO 228
      L=1
      EL=1.
      SIGMSQ=SIGMA(ISB)*SIGMA(ISB)*FACTOR*FACTOR
C
C        2. CALCULATE TRIAL ELASTIC STRESS INCREMENTS
C
      DELSIG(1)=A1*DELEPS(1) + B1*(DELEPS(2)+DELEPS(3))
      DELSIG(2)=A1*DELEPS(2) + B1*(DELEPS(1)+DELEPS(3))
      DELSIG(3)=A1*DELEPS(3) + B1*(DELEPS(1)+DELEPS(2))
      DELSIG(4)=C1*DELEPS(4)
      DELSIG(5)=C1*DELEPS(5)
      DELSIG(6)=C1*DELEPS(6)
C
   45 LC=1
   50 SUBINC=1./EL
C        3. CALCULATE TRIAL ELASTIC STRESSES
C
      DO 60 I=1,6
      TR(I)=TM(I)+DELSIG(I)*SUBINC
   60 CONTINUE
      TAUR=TR(1)+TR(2)+TR(3)
C
C        4. CHECK THROUGH VON MISES-HENCKY YIELD CRITERIA
C           YIELD PHI
      CZ=TR(1)**2+TR(2)**2+TR(3)**2+2.0*(TR(4)**2+TR(5)**2+TR(6)**2)-
     1(TAUR**2+2.0*SIGMSQ)/3.0
C
C         TEST YIELD CONDITION
C
      HLAMDA=0.0
      IF(CZ.LE.0. .AND. L .EQ.1)GOTO 215
      IF(CZ .LE. 0.)GOTO 110
C
C        5. COMPUTE NECESSARY CORRECTOR
C
      SM=(TM(1)+TM(2)+TM(3))/3.0
      TC(1)=TM(1)-SM
      TC(2)=TM(2)-SM
```

```
      TC(3)=TM(3)-SM
      TC(4)=TM(4)
      TC(5)=TM(5)
      TC(6)=TM(6)
      TAUC=TC(1)+TC(2)+TC(3)
C
C        6. CALCULATE PLASTICITY PARAMETER FROM HUFFINGTON MODEL
C
      AZ=TC(1)**2+TC(2)**2+TC(3)**2+2.0*(TC(4)**2+TC(5)**2+TC(6)**2)
     1   -(TAUC**2/3.0)
      BZ=TC(1)*TR(1)+TC(2)*TR(2)+TC(3)*TR(3)+2.0*(TR(4)*TC(4)+
     1   TR(5)*TC(5)+TR(6)*TC(6))-TAUC*TAUR/3.0
      DISCR=BZ*BZ-AZ*CZ
C
C           TEST AZ
C          IF AZ IS NEGATIVE - PRINT ERROR MESSAGE
C          IF AZ IS ZERO     - SUB-INCREMENT
C          IF AZ IS POSITIVE - CONTINUE
C
      IF(AZ) 80,150,100
   80 WRITE(6,90)
   90 FORMAT('3',4X,'AZ NEGATIVE AT'/)
      GOTO 180
C
C          TEST DISCRIMINANT
C        IF DISCR IS NEGATIVE SUB-INCREMENT
C
  100 IF(DISCR .LT. 0.0)GOTO 150
C
C          TEST BZ
C        IF BZ IS NEGATIVE OR ZERO SUB-INCREMENT
C
      IF(BZ .LE. 0.0)GOTO 150
C          COMPUTE HLAMBDA
      HLAMDA=CZ/(BZ+SQRT(DISCR))
C        7. EVALUATE SUBLAYER RELIEVED ELASTIC STRESSES
C
  110 DO 120 I=1,6
      TM(I)=TR(I)-HLAMDA*TC(I)
  120 CONTINUE
C
C
C          CHECK THE SUB-INCREMENT NUMBER
C
      IF(LC.EQ.L) GOTO 210
      LC=LC+1
      GO TO 50
C
C          MAKE SUB-INCREMENTS SMALLER
C
  150 L=L+1
      EL=L
C
C          CHECK MAXIMUM NUMBER OF ALLOWABLE SUB-INCREMENTS
```

```
      IF(L .LE. 100)GOTO 45
      WRITE(6,170)
  170 FORMAT('3STRESS CALCULATION UNSATISFACTORY(100 SUB-INCREMENTS)
     1 /)
  180 WRITE(6,3000) ISH,L,LC,NEL,IPT,TIME
 3000 FORMAT(' SUBLAYER=',I4,' SUB-INCREMMENT L=',I4,' LC=',I4,
     1' ELEMENT NUMBER=',I4,' IPOINT=',I4,' TIME=',E15.8)
      WRITE(6,3005) CZ,AZ,BZ
 3005 FORMAT(' CZ=',E15.8,' AZ=',E15.8,' BZ=',E15.8)
      WRITE(6,3010) (SIG(ISB,I),I=1,6)
 3010 FORMAT(' SIG(ISB,I) ',6E15.8)
      WRITE(6,3020) (TR(I),I=1,6)
 3020 FORMAT(' TR ',6E15.8)
      WRITE(6,3021) (TC(I),I=1,6)
 3021 FORMAT(' TC ',6E15.8)
      WRITE(6,3022) (TM(I),I=1,6)
 3022 FORMAT(' TM ',6E15.8)
      WRITE(6,3023) (DELSIG(I),I=1,6)
 3023 FORMAT(' DELSIG ',6E15.8)
      STOP 'STRESS CALCULATION UNSATISFACTORY'
C              REACHED PLASTIC SOLUTION
  210 IPLAST=IPLAST+1
      GOTO 225
C        ELASTIC TM EQUALS TRIAL TR PER SUBLAYER
  215 DO 220 I=1,6
      TM(I)=TR(I)
  220 CONTINUE
C     STRESS ROTATION IS APPLIED IN LARGE DISPLACEMENT/STRAIN
C
  225 IF(INDNL.NE.3)GOTO 226
      OMEGA1=DISD(4)-DISD(6)
      OMEGA2=DISD(5)-DISD(8)
      OMEGA3=DISD(7)-DISD(9)
      TM(1)=TM(1)+SIG(ISB,4)*OMEGA1+SIG(ISB,5)*OMEGA2
      TM(2)=TM(2)-SIG(ISB,4)*OMEGA1+SIG(ISB,6)*OMEGA3
      TM(3)=TM(3)-SIG(ISB,5)*OMEGA2-SIG(ISB,6)*OMEGA3
      TM(4)=TM(4)+.5*(OMEGA1*(SIG(ISB,2)-SIG(ISB,1))+
     1              OMEGA3*SIG(ISB,5)+OMEGA2*SIG(ISB,6))
      TM(5)=TM(5)+.5*(OMEGA2*(SIG(ISB,3)-SIG(ISB,1))+
     1              OMEGA1*SIG(ISB,6)-OMEGA3*SIG(ISB,4))
      TM(6)=TM(6)+.5*(OMEGA3*(SIG(ISB,3)-SIG(ISB,2))-
     1              OMEGA2*SIG(ISB,4)-OMEGA1*SIG(ISB,5))
  226 IF(IUPDT .NE. 0)GOTO 228
C
C        STORE SUBLAYER STRESS TM(I) IN SIG(ISB,I) FOR NEXT STEP
C
      DO 227 I=1,6
      SIG(ISB,I)=TM(I)
  227 CONTINUE
C
C        8. CALCULATE TOTAL STRESSES FROM SUBLAYER STRESS
C
  228 DO 230 I=1,6
      STRESS(I)=STRESS(I)+TM(I)*COEFF(ISH)
  230 CONTINUE
```

```
  250 CONTINUE
C
C     .....  CALCULATION OF ELASTIC-PLASTIC STRESSES  .....(E N D
      IF(KPRI .EQ. 0)GOTO 700
      IPELD=1
      IF(IPLAST .GT. 0)IPELD=2
C
C     U P D A T I N G
C
      IF (IUPDT.NE.0)GOTO 615
      IPEL=IPELD
      DO 610 I=1,6
  610 EPS(I)=STRAIN(I)
C
  615 RETURN
C
C     PRINTING OF STRESSES
C
  700 IF (IPRI.EQ.0 .AND. IPT.EQ.1) WRITE (6,2100) NEL
C        9. CALCULATE HYDROSTATIC AND DEVIATORIC STRESSES
C
      SM=(STRESS(1)+STRESS(2)+STRESS(3))/3.0
      SX=STRESS(1)-SM
      SY=STRESS(2)-SM
      SZ=STRESS(3)-SM
      FTA=.5 * (SX**2+SY**2+SZ**2) +
     1    STRESS(4)**2 + STRESS(5)**2 + STRESS(6)**2
      FTA=SQRT(3.*FTA)
      IF (INUNL.NE.2) GO TO 800
C
C     IN TOTAL LAGRANGIAN FORMULATION CALCULATE CAUCHY STRESSES
C
      IF (IPRI.EQ.0)
     1 WRITE (6,2200) IPT,STATE(IPELD),STRESS,FTA,L,LC
      CALL CAUCH3
C
  800 IF (IPRI.EQ.0)
     1 WRITE (6,2200) IPT,STATE(IPELD),STRESS,FTA,L,LC
      RETURN
 2100 FORMAT (/16H ELEMENT  STRESS,90X,10HEQUIVALENT/
     1       13H NUM/IPT   STATE      STRESS-XX     STRESS-YY
     2S-ZZ     STRESS-XY     STRESS-XZ     STRESS-YZ        STRESS
     3L       LC /I4)
 2200 FORMAT (5X,I2,1X,A2,6HLASTIC,1X,6E14.6,1X,E14.6,3X,I3,5X,I3)
```

LIST OF SYMBOLS

D^{α}, N^{α}	empirically determined constants in the strain rate equation.
E	Young's modulus (GPa).
E_T	tangent strain hardening modulus (GPa).
S_{ij}^{α}	deviatoric stress tensor at the αth sublayer.
δ_{ij}	Kronecker delta.
$\dot{\varepsilon}^2$	second invariant of the deviatoric strain rate tensor.
ε_{ij}	physical strain at a point.
ε_{kk}	hydrostatic components of strain.
ν	Poisson's ratio.
ρ	mass density (Kg/m^3).
σ_{ij}	physical stress at a point (MPa).
σ_{kk}	hydrostatic components of the sublayer stress (MPa).
$\sigma_{ij}^{\alpha}(n)$	sublayer stress at the αth sublayer at the current cycle (MPa).
$\sigma_{ij}^{\alpha}(n-1)$	sublayer stress at the αth sublayer at the previous cycle (MPa).
$\sigma_{ij}^{T\alpha}$	trial sublayer stress (MPa).
σ_y	sublayer yield stress (MPa).
σ_o^{α}	static sublayer yield stress (MPa).
ϕ	von Mises yield function.
ω	sublayer weighting factor.
$\Delta\varepsilon_{ij}$	strain increment.
$\Delta\lambda^{\alpha}$	plastic flow parameter.
$\Delta\sigma_{ij}^{\alpha}$	sublayer stress increment (MPa).
$\Delta\sigma_{ij}$	elastic stress increment (MPa).

DISTRIBUTION LIST

No. of Copies	Organization
12	Defense Technical Info Center ATTN: DTIC-DDA Cameron Station Alexandria, VA 22314
1	Director of Defense Research & Engineering ATTN: DD/TWP Washington, DC 20301
1	Asst. to the Secretary of Defense (Atomic Energy) ATTN: Document Control Washington, DC 20301
1	Director Defense Advanced Research Projects Agency ATTN: Tech Lib 1400 Wilson Boulevard Arlington, VA 22209
2	Director Federal Emergency Management Agency ATTN: Mr. George Sisson/RF-SR Technical Library Washington, DC 20301
1	Director Defense Intelligence Agency ATTN: DT-2/Wpns & Sys Div Washington, DC 20301
1	Director National Security Agency ATTN: E. F. Butala, R15 Ft. George G. Meade, MD 20755
1	Director Joint Strategic Target Planning Staff JCS Offut AFB Omaha, NB 68113
1	Director Defense Communications Agency ATTN: 930 Washington, DC 20305
5	Director Defense Nuclear Agency ATTN: STSI/Archives SPAS STSP STVL/Dr. La Vier RATN Washington, DC 20305
6	Director Defense Nuclear Agency ATTN: DDST/Dr. Conrad SSTL/Tech Lib (2 cys) SPSS/K. Goering G. Ullrich SPTD/T. Kennedy Washington, DC 20305
2	Commander Field Command, DNA ATTN: FCPR FCTMOF Kirtland AFB, NM 87115
1	Commander Field Command, DNA Livermore Branch ATTN: FCPRL P.O. Box 808 Livermore, CA 94550
1	Director Inst for Defense Analyses ATTN: Library 1801 Beauregard St. Alexandria, VA 22311
1	Commander US Army Materiel Development and Readiness Command ATTN: DRCDMD-ST 5001 Eisenhower Avenue Alexandria, VA 22333

DISTRIBUTION LIST

No. of Copies	Organization
1	Program Manager US Army BMD Program Office ATTN: John Shea 5001 Eisenhower Avenue Alexandria, VA 22333
2	Director US Army BMD Advanced Technology Center ATTN: CRDABH-X CRDABH-S Huntsville, AL 35804
1	Commander US Army BMD Command ATTN: BDMSC-TFN/N.J. Hurst P.O. Box 1500 Huntsville, AL 35804
2	Deputy Chief of Staff for Operations and Plans ATTN: Technical Library Director of Chemical & Nuc Operations Department of the Army Washington, DC 20310
2	Office, Chief of Engineers Department of the Army ATTN: DAEN-MCE-D DAEN-RDM 890 South Pickett Street Alexandria, VA 22304
3	Commander US Army Engineer Waterways Experiment Station ATTN: Technical Library William Flathau Leo Ingram P.O. Box 631 Vicksburg, MS 39181
1	Commander US Army Engineer School ATTN: ATSE-CD Fort Belvoir, VA 22060
1	Commander US Army MERADCOM ATTN: DRDME-EM, D. Frink Fort Belvoir, VA 22060
1	Commander US Army Materiel Development and Readiness Command ATTN: DRCDMD-ST, N. Klein 5001 Eisenhower Avenue Alexandria, VA 22333
1	Commander US Army Armament Research and Development Command ATTN: DRDAR-TDC, Dr. Gyorog Dover, NJ 07801
3	Commander US Army Armament Research and Development Command ATTN: DRDAR-LCN-F, W. Reiner DRDAR-TSS Dover, NJ 07801
1	Commander US Army Armament Materiel Readiness Command ATTN: DRSAR-LEP-L Rock Island, IL 61299
1	Director US Army ARRADCOM Benet Weapons Laboratory ATTN: DRDAR-LCB-TL Watervliet, NY 12189
1	Commander US Army Aviation Research and Development Command ATTN: DRDAV-E 4300 Goodfellow Boulevard St. Louis, MO 63120

DISTRIBUTION LIST

No. of Copies	Organization
1	Director US Army Air Mobility Research and Development Laboratory Ames Research Center Moffett Field, CA 94035
1	Commander US Army Communications Rsch and Development Command ATTN: DRSEL-ATDD Fort Monmouth, NJ 07703
3	Commander US Army Electronics Research and Development Command ATTN: DELSD-L DELEW-E, W. S. McAfee DELSD-EI, J. Roma Fort Monmouth, NJ 07703
8	Commander US Army Harry Diamond Labs ATTN: Mr. James Gaul Mr. L. Belliveau Mr. J. Meszaros Mr. J. Gwaltney Mr. F. W. Balicki Mr. Bill Vault Mr. R. J. Bostak Mr. R. K. Warner 2800 Powder Mill Road Adelphi, MD 20783
4	Commander US Army Harry Diamond Labs ATTN: DELHD-TA-L DRXDO-TI/002 DRXDO-NP DELHD-RBA/J. Rosado 2800 Powder Mill Road Adelphi, MD 20783
2	Commandant US Army Infantry School ATTN: ATSH-CD-CSO-OR Fort Benning, GA 31905
1	Commander US Army Missile Command ATTN: DRSMI-YDL Redstone Arsenal, AL 35898
1	Commander US Army Missile Command ATTN: DRSMI-R Redstone Arsenal, AL 35898
4	Commander US Army Natick Research and Development Command ATTN: DRDNA-DT, Dr. D. Sieling DRXNE-UE/A. Johnson A. Murphy W. Crenshaw Natick, MA 01762
1	Commander US Army Tank Automotive Command ATTN: DRSTA-TSL Warren, MI 48090
1	Commander US Army Foreign Science and Technology Center ATTN: Rsch & Concepts Br 220 7th Street, NE Charlottesville, VA 22901
1	Commander US Army Logistic ATTN: ATCL-O Mr. Robert Cameron Fort Lee, VA 23801
3	Commander US Army Materials and Mechanics Research Center ATTN: Technical Library DRXMR-ER, Joe Prifti Eugene de Luca Watertown, MA 02172

DISTRIBUTION LIST

No. of Copies	Organization
1	Commander US Army Research Office P.O. Box 12211 Research Triangle Park NC 27709
4	Commander US Army Nuclear & Chem Agency ATTN: ACTA-NAW MONA-WE Technical Library MAJ Uecke 7500 Backlick Rd, Bldg. 2073 Springfield, VA 22150
1	Commander US Army TRADOC ATTN: ATCD-SA Fort Monroe, VA 23651
2	Director US Army TRADOC Systems Analysis Activity ATTN: LTC John Hesse ATAA-SL White Sands Missile Range NM 88002
1	Commander US Combined Arms Combat Developments Activity ATTN: ATCA-CO, Mr. L. C. Pleger Fort Leavenworth, KS 66027
1	Commandant Interservice Nuclear Weapons School ATTN: Technical Library Kirtland AFB, NM 87115
1	Chief of Naval Material ATTN: MAT 0323 Department of the Navy Arlington, VA 22217
2	Chief of Naval Operations ATTN: OP-03EG OP-985F Department of the Navy Washington, DC 20350
1	Chief of Naval Research ATTN: N. Perrone Department of the Navy Washington, DC 20360
1	Director Strategic Systems Projects Ofc ATTN: NSP-43, Tech Lib Department of the Navy Washington, DC 20360
1	Commander Naval Electronic Systems Com ATTN: PME 117-21A Washington, DC 20360
1	Commander Naval Facilities Engineering Command Washington DC 20360
1	Commander Naval Sea Systems Command ATTN: ORD-91313 Library Department of the Navy Washington, DC 20362
3	Officer-in-Charge (Code L31) Civil Engineering Laboratory Naval Constr Btn Ctr ATTN: Stan Takahashi R. J. Odello Technical Library Port Hueneme, CA 93041
1	Commander David W. Taylor Naval Ship Research & Development Ctr ATTN: Lib Div, Code 522 Bethesda, MD 20084

DISTRIBUTION LIST

No. of Copies	Organization
1	Commander Naval Surface Weapons Center ATTN: DX-21, Library Br. Dahlgren, VA 22448
2	Commander Naval Surface Weapons Center ATTN: Code WA501/Navy Nuclear Programs Office Code WX21/Tech Lib Silver Spring, MD 20910
1	Commander Naval Weapons Center ATTN: Code 3431, Tech Lib China Lake, CA 93555
1	Commander Naval Weapons Evaluation Fac ATTN: Document Control Kirtland Air Force Base Albuquerque, NM 87117
1	Commander Naval Research Laboratory ATTN: Code 2027, Tech Lib Washington, DC 20375
1	Superintendent Naval Postgraduate School ATTN: Code 2124, Technical Reports Library Monterey, CA 93940
1	AFSC (SDOA/Tech Lib) Andrews Air Force Base Washington, DC 20334
1	ADTC (DLODL) Eglin AFB, FL 32542
1	AFATL (DLYV) Eglin AFB, FL 32542
1	RADC (EMTLD/Docu Library) Griffiss AFB, NY 13340
1	AFWL/NTES (R. Henny) Kirtland AFB, NM 87115
1	AFWL/NTE, CPT J. Clifford Kirtland AFB, NM 87115
1	Commander-in-Chief Strategic Air Command ATTN: NRI-STINFO Lib Offutt AFB, NB 68113
1	AFIT (Lib Bldg. 640, Area B) Wright-Patterson AFB Ohio 45433
1	FTD (NIIS) Wright-Patterson AFB Ohio 45433
1	Director Lawrence Livermore Lab ATTN: Tech Info Dept L-3 P.O. Box 808 Livermore, CA 94550
1	Director Los Alamos Scientific Lab ATTN: Doc Control for Rpts Lib P.O. Box 1663 Los Alamos, NM 87544
2	Sandia Laboratories ATTN: Doc Control for 3141 Sandia Rpt Collection L. J. Vortman Albuquerque, NM 87115
1	Sandia Laboratories Livermore Laboratory ATTN: Doc Control for Tech Lib P.O. Box 969 Livermore, CA 94550

DISTRIBUTION LIST

No. of Copies	Organization
1	Director National Aeronautics and Space Administration Scientific & Tech Info Fac P.O. Box 8757 Baltimore/Washington International Airport MD 21240
1	Aerospace Corporation ATTN: Tech Info Services P.O. Box 92957 Los Angeles, CA 90009
1	Agbabian Associates ATTN: M. Agbabian 250 North Nash Street El Segundo, CA 90245
1	The BDM Corporation ATTN: Richard Hensley P.O. Box 9274 Albuquerque International Albuquerque, NM 87119
1	The Boeing Company ATTN: Aerospace Library P.O. ox 3707 Seatle, WA 98124
1	Goodyear Aerospace Corp ATTN: R. M. Brown, Bldg 1 Shelter Engineering Litchfield Park, AZ 85340
5	Kaman AviDyne ATTN: Dr. N.P. Hobbs (4 cys) Mr. S. Criscione 83 Second Avenue Northwest Industrial Park Burlington, MA 01830
3	Kaman Nuclear ATTN: Library P. A. Ellis F. H. Shelton 1500 Garden of the Gods Road Colorado Springs, CO 80907
1	Kaman Sciences Corporation ATTN: Don Sachs Suite 703 2001 Jefferson Davis Highway Arlington, VA 22202
1	Kaman-TEMPO ATTN: DASIAC P.O. Drawer QQ Santa Barbara, CA 93102
1	Kaman-TEMPO ATTN: E. Bryant, Suite UL-1 715 Shamrock Road Bel Air, MD 21014
1	Lockheed Missiles & Space Co. ATTN: J. J. Murphy, Dept. 81-11 Bldg. 154 P.O. Box 504 Sunnyvale, CA 94086
1	Martin Marietta Aerospace Orlando Division ATTN: G. Fotieo P.O. Box 5837 Orlando, FL 32805
2	McDonnell Douglas Astronautics Corporation ATTN: Robert W. Halprin Dr. P. Lewis 5301 Bolsa Avenue Huntington Beach, CA 92647
2	The Mitre Corporation ATTN: Library J. Calligeros, Mail Stop B-150 P.O. Box 208 Bedford, MA 01730
1	Pacific Sierra Research Corp ATTN: Dr. Harold Brode 1456 Cloverfield Boulevard Santa Monica, CA 90404

DISTRIBUTION LIST

No. of Copies	Organization
1	Physics International Corp 2700 Merced Street San Leandro CA 94577
1	Radkowski Associates ATTN: Peter R. Radkowski P.O. Box 5474 Riverside, CA 92517
4	R&D Associates ATTN: Jerry Carpenter J. G. Lewis Technical Library Allan Kuhl P.O. Box 9695 Marina del Rey, CA 90291
1	RCA Government Communications Systems 13-5-2 Front & Copper Streets Camden, NJ 08102
2	Science Applications, Inc. ATTN: Burton S. Chambers John Cockayne P.O. Box 1303 1710 Goodridge Drive McLean, VA 22102
1	Science Applications, Inc. ATTN: Technical Library P.O. Box 2351 La Jolla, CA 92038
1	Science Systems and Software ATTN: C. E. Needham P.O. Box 8243 Albuquerque, NM 87198
1	Systems Science and Software ATTN: Technical Library P.O. Box 1620 La Jolla, CA 92037
1	TRW Systems Group ATTN: Benjamin Sussholtz One Space Park Redondo Beach, CA 92078
2	Union Carbide Corporation Holifield National Laboratory ATTN: Doc Control for Tech Lib Civil Defense Rsch Project P.O. Box X Oak Ridge, TN 37830
1	Weidlinger Assoc. Consulting Engineers ATTN: M. L. Baron 110 East 59th Street New York, NY 10022
1	Battelle Memorial Institute ATTN: Technical Library 505 King Avenue Columbus, OH 43201
1	California Inst of Tech ATTN: T. J. Ahrens 1201 E. California Blvd. Pasadena, CA 91109
2	Denver Reseach Institute University of Denver ATTN: Mr. J. Wisotski Technical Library P.O. Box 10127 Denver, CO 80210
1	IIT Research Institute ATTN: Milton R. Johnson 10 West 35th Street Chicago, IL 60616
1	J. D. Haltiwanger Consulting Services B106a Civil Engineering Bldg. 208 N. Romine Street Urbana, IL 61801

DISTRIBUTION LIST

No. of Copies	Organization
1	Massachusetts Institute of Technology Aeroelastic and Structures Research Laboratory ATTN: Dr. E. A. Witmer Cambridge, MA 02139
1	Massachusetts Institute of Technology Mechanical Engineering Dept ATTN: Prof. K. J. Bathe Cambridge, MA 02139
2	Southwest Research Institute ATTN: Dr. W. E. Baker A. B. Wenzel 8500 Culebra Road San Antonio, TX 78228
1	SRI International ATTN: Dr. G. R. Abrahamson 333 Ravenswood Avenue Menlo Park, CA 94025
1	Stanford University ATTN: Dr. D. Bershader Durand Laboratory Standord, CA 94305
1	Washington State University Physics Department ATTN: G. R. Fowles Pullman, WA 99163

No. of Copies	Organization
	Dir, USAMSAA ATTN: DRXSY-D DRXSY-MP, H.Cohen
	Cdr, USATECOM ATTN: DRSTE-TO-F
	Dir, USACSL Bldg. E3516, EA ATTN: DRDAR-CLB-PA DRDAR-CLN DRDAR-CLJ-L

USER EVALUATION OF REPORT

Please take a few minutes to answer the questions below; tear out this sheet, fold as indicated, staple or tape closed, and place in the mail. Your comments will provide us with information for improving future reports.

1. BRL Report Number _____

2. Does this report satisfy a need? (Comment on purpose, related project, or other area of interest for which report will be used.)

_____

_____

_____

3. How, specifically, is the report being used? (Information source, design data or procedure, management procedure, source of ideas, etc.) _____

_____

_____

4. Has the information in this report led to any quantitative savings as far as man-hours/contract dollars saved, operating costs avoided, efficiencies achieved, etc.? If so, please elaborate.

_____

_____

5. General Comments (Indicate what you think should be changed to make this report and future reports of this type more responsive to your needs, more usable, improve readability, etc.) _____

_____

_____

_____

6. If you would like to be contacted by the personnel who prepared this report to raise specific questions or discuss the topic, please fill in the following information.

Name: _____

Telephone Number: _____

Organization Address: _____

_____

_____

FOLD HERE

Director
US Army Ballistic Research Laboratory
ATTN: DRDAR-BLA-S
Aberdeen Proving Ground, MD 21005

NO POSTAGE
NECESSARY
IF MAILED
IN THE
UNITED STATES

OFFICIAL BUSINESS
PENALTY FOR PRIVATE USE, $300

BUSINESS REPLY MAIL
FIRST CLASS PERMIT NO 12062 WASHINGTON, DC
POSTAGE WILL BE PAID BY DEPARTMENT OF THE ARMY

Director
US Army Ballistic Research Laboratory
ATTN: DRDAR-BLA-S
Aberdeen Proving Ground, MD 21005

FOLD HERE